[1] G. Borrman, Phys. Z. **42**, 157 [1941].
[2] M. von Laue, Acta Cryst. **2**, 106 [1949].
[3] G. Honjo, J. Phys. Soc. Japan **8**, 776 [1953].
[4] G. Honjo and K. Mihama, J. Phys. Soc. Japan **9**, 184 [1954].
[5] K. Kohra and H. Watanabe, J. Phys. Soc. Japan **14**, 1119 [1959].
[6] H. Hashimoto, A. Howie, and M. J. Whelan, Phil. Mag. **5**, 967 [1960].
[7] H. Hashimoto, A. Howie, and M. J. Whelan, Proc. Roy. Soc. London A **269**, 80 [1962].
[8] P. B. Hirsch, A. Howie, R. B. Nicholson, D. W. Pashley, and M. J. Whelan, "Electron Microscopy of Thin Crystals, Butterworths, London 1965.
[9] C. J. Humphreys and P. B. Hirsch, Phil. Mag. **18**, 115 [1968].
[10] G. Radi, Acta Cryst. A **26**, 41 [1969].
[11] P. B. Hirsch, A. Howie, and M. J. Whelan, Phil. Mag. **7**, 2095 [1962].
[12] P. Duncumb, Phil. Mag. **7**, 2101 [1962].
[13] C. R. Hall, Proc. Roy. Soc. A **295**, 140 [1966].
[14] D. W. Pashley, Phil. Mag. **4**, 324 [1959].
[15] C. J. Cooke and I. K. Openshaw, Proc. IV National Conf. on Electron Microprobe Analysis (Pasadena — Electron Probe Analysis Soc. of America) paper 64 [1969].
[16] M. J. Whelan, J. Appl. Phys. **36**, 2099 [1965].
[17] R. D. Heidenreich, J. Appl. Phys. **33**, 2321 [1962].
[18] C. R. Hall, Phil. Mag. **22**, 63 [1970].
[19] D. R. Clarke and A. Howie, Phil. Mag. **24**, 959 [1971].
[20] J. P. Spencer, C. J. Humphreys, and P. B. Hirsch, Phil. Mag. **26**, 193 [1972].
[21] E. Vicario, M. Pitaval, and G. Fontaine, Proc. 7th Internat. E. M. Conf. (Grenoble) **2**, 211 [1970].
[22] L. Reimer, H. G. Badde, H. Seidel, and W. Bühring, Z. angew. Phys. **31**, 145 [1971].

Absorption and Penetration in the Semi-classical Theory of High Energy Electron Diffraction

P. A. Doyle and M. V. Berry

H. H. Wills Physics Laboratory, University of Bristol, United Kingdom

(Z. Naturforsch. **28 a**, 571—576 [1973]; received 22 January 1973)

Dedicated to Professor Dr. G. Borrmann on his 65th birthday

The approximations under which the effect of inelastic scattering on the elastic scattering of electrons can be described by the use of a complex potential are discussed. Within these approximations, inelastic scattering is incorporated in the semi-classical theory for high energy electron diffraction. A simple explanation is given for the voltage and orientation at which maximum penetration is achieved for thick crystals. Good agreement is obtained between the predictions of this semi-classical theory and those of the conventional quantum mechanical approach for gold (111) systematics.

1. Introduction

A number of theories for the dynamical scattering of fast charged particles by crystals have been given [1–5]. Recently, Berry [6] (hereafter called I) developed a semi-classical approximation for elastic scattering. This treatment becomes increasingly valid at higher accelerating voltages, for which the greater number of interacting beams renders alternative approaches more difficult to handle numerically.

Inelastic scattering has been included phenomenologically in dynamical theories for electrons [7, 8] by the use of a complex potential. This complex potential gives an account of the phenomenon of Bloch wave channeling, just as the use of a complex structure factor describes the Borrmann effect [9, 10] for X-rays. The aproximations under which this potential is valid were described by Yoshioka [11] and by Radi [12]. We make use of the work of these authors to discuss the effect of the inelastic on the elastic scattering of electrons, using the semi-classical theory of I. In this approach the wave functions are studied in real space, which enables an understanding to be obtained of the physical origin of channelling for different Bloch waves; in addition, the method results in simple analytical formulae, and is thus complementary to the conventional many beam computational techniques [8]. Particular attention is paid to an explanation of the voltage and orientation which maximize electron penetration of thick specimens.

Reprint requests to Dr. P. A. Doyle, H. H. Wills Physics Laboratory, Royal Fort — Tyndall Avenue, University of Bristol, *Bristol BS8 1TL*/England.

2. The Complex Potential in Electron Diffraction

Consider an electron of kinetic energy eE, wave vector $\boldsymbol{k}_0$ and relativistic mass m incident on a crystal of volume V, which can exist in excited states n.

Let $H_{nm}(\boldsymbol{r})$ be matrix elements of the Hamiltonian for the Coulomb interaction between the incident electron and the crystal electrons and nuclei. To a good approximation, the diagonal elements $H_{nn}(\boldsymbol{r})$ are proportional to the crystal potential $\mathcal{V}^r(\boldsymbol{r})$, so that

$$H_{nn}(\boldsymbol{r}) = H_{00}(\boldsymbol{r}) = (2me/\hbar^2)\,\mathcal{V}^r(\boldsymbol{r}) = -(2me/\hbar^2)\sum_g \mathcal{V}_g^{\,r}\exp\{i\boldsymbol{g}\cdot\boldsymbol{r}\}\,. \tag{1}$$

Radi [12] included dynamical interactions for inelastic as well as for elastic waves in the crystal, requiring each inelastic wave to be weak compared to the elastic wave. Omitting transitions of the type $m \neq n$ with m and n both non-zero, he found that the dispersion equations for the Bloch wave coefficients χ_g of the elastic wave function $\Psi(\boldsymbol{r})$ could be written as

$$\sum_g [(2me/\hbar^2)\,\mathcal{V}_{g-h}^{\,r} - C_{hg} + (k_0^2 - \boldsymbol{K}_h^2)\,\delta_{hg}]\,\chi_g = 0 \tag{2}$$

where

$$C_{hg} = \sum_{n\neq 0}^{\infty}(1/V)\int_V\int_V \mathrm{d}\boldsymbol{r}\,\mathrm{d}\boldsymbol{r}'\exp\{-i\boldsymbol{K}_h\cdot\boldsymbol{r}\}\,H_{0n}(\boldsymbol{r})\,G^+(\boldsymbol{r},\boldsymbol{r}';k_n)\,H_{n0}(\boldsymbol{r}')\exp\{i\boldsymbol{K}_g\cdot\boldsymbol{r}'\}\,. \tag{3}$$

The energy of state n is $(eE - \hbar^2 k_n^2/2m)$. The Green function $G^+(\boldsymbol{r},\boldsymbol{r}';k_n)$ is constructed from a Bloch function which describes the inelastically scattered wave when the crystal is excited to state n. Equations (2) are solved for χ_g and the allowed wave vectors $\boldsymbol{K}$ in the crystal, where $\boldsymbol{K}_g = \boldsymbol{K} + \boldsymbol{g}$. These allowed values form the dispersion surfaces, which are characterized by a parameter j.

Suppose that the inelastic interaction is localized within a sphere of radius r_0 about each atom. Then the integral over $\boldsymbol{r}'$ in Eq. (3) for $|\boldsymbol{r}-\boldsymbol{r}'| > r_0$ gives zero contribution to C_{hg}. If $r_0|\boldsymbol{h}| \ll 2\pi$ for all reflections $\boldsymbol{h}$ included, it readily follows that C_{hg} depends only on $|\boldsymbol{g}-\boldsymbol{h}|$, i. e., $C_{hg} \equiv C_{0,g-h}$. The Green function goes over to that for an outgoing spherical wave, and the dispersion Eqs. (2) reduce to those derived earlier by Yoshioka [11]. This localized approximation holds for the excitation of core electrons on a tight binding model, and of thermal vibrations on an Einstein model. The excitation of plasmons is not a localized interaction. However, ignoring the effect of the periodic ion core on the valence or conduction electrons, it follows [12] that $C_{hg}(\text{plasmon}) = 0$ if $h \neq g$. Since $C_{gg} = C_{00}$, the plasmon contribution to C_{hg} can be written in the form $C_{0,g-h}\,\delta_{hg}$. Therefore, within the approximations stated for the three principal inelastic scattering processes * we can include C_{hg} in Eqs. (2) by allowing $\mathcal{V}_{g-h}^{\,r}$ to become complex. Thus

$$\mathcal{V}_g^{\,r} \to \mathcal{V}_g^{\,r} + i\,\mathcal{V}_g^{\,i} \tag{4}$$

where $\mathcal{V}_g^{\,i}$, defined as $(\hbar^2/2me)\,\mathrm{Im}(C_{0g})$, is a small imaginary contribution to the potential, whose magnitude is greatest near the atoms, and which is negative in sign. The real parts of C_{0g} represent virtual inelastic processes, and will be omitted. Yoshioka [11] discussed the importance of these real parts in the interpretation of observed lattice potentials $\mathcal{V}_g^{\,r}$.

* Bremsstrahlung becomes important only at very high energies and is not considered here. Ohtaka, Ohtsuki and Yanagawa [13] show that it is negligible up to at least 2 MeV.

3. Theory

We have considered the standard treatment of the scattering in order to state clearly the approximations under which the effect of the inelastic on the elastic electron scattering can be included by using a complex potential. The semi-classical theory of I began with the Schrödinger equation

$$[\nabla^2 + k_0^2 - U(\boldsymbol{r})]\,\Psi(\boldsymbol{r}) = 0 \tag{5}$$

where the reduced potential $U(\boldsymbol{r})$ is now given by

$$\begin{aligned} U(\boldsymbol{r}) &\equiv U^r(\boldsymbol{r}) + i\,U^i(\boldsymbol{r}) \\ &= (2me/\hbar^2)\,[\mathcal{V}^r(\boldsymbol{r}-\boldsymbol{a}/2) + i\,\mathcal{V}^i(\boldsymbol{r}-\boldsymbol{a}/2)]\,. \end{aligned} \tag{6}$$

The unit cell has dimensions $\boldsymbol{a} = (a, b, c)$. The reason for the different choice of origin for $U(\boldsymbol{r})$ will become apparent below. We write the co-ordinate $\boldsymbol{r}$ as $(\boldsymbol{R}, z)$ and define $\boldsymbol{K}_0$ as the projection of $\boldsymbol{k}_0$ in the $\boldsymbol{R}$ plane (see Figure 1).

The analysis given in I which leads to a simplification of Eq. (5) can be followed exactly with the complex $U(\boldsymbol{r})$. For high energies ($\gtrsim 100$ keV) and simple crystal structures, the wave propagation proceeds according to the phase grating approximation [14] over distances equal to at least one lattice spacing, and this implies that the z-dependence of $U(\boldsymbol{r})$ does not influence the solutions of Equation (5). Thus $U(\boldsymbol{r})$ can be replaced by its average over the z-direction, $\bar{U}(\boldsymbol{R})$. This approximation is equivalent to omitting upper and lower layer lines from

a dynamical calculation, and as shown in I, results in the z-co-ordinate behaving like a time co-ordinate. Defining $\mathcal{T}(\boldsymbol{R}, z)$ by

$$\mathcal{T}(\boldsymbol{R}, z) = \Psi(\boldsymbol{r}) \exp\{-i z (k_0^2 - K_0^2)^{1/2}\} \quad (7)$$

it follows from Eq. (5) that

$$[\nabla_{\boldsymbol{R}}^2 + K_0^2 - U(\boldsymbol{R})]\, \mathcal{T}(\boldsymbol{R}, z) = -2 i k \cdot \partial \mathcal{T}(\boldsymbol{R}, z)/\partial z . \quad (8)$$

Equation (8) ignores back-scattering, and a "Fresnel" approximation has been made for the propagation of forward scattered waves.

With $\bar{U}(\boldsymbol{R})$ replaced by its real part only, Eq. (8) is exactly Eq. (30) of I, for which the solutions are

$$\mathcal{T}(\boldsymbol{R}, z) = \left[\sum_j B_j \mathcal{T}_j(\boldsymbol{R}) \exp\{-i s_j^r z/2k\}\right] \exp\{i K_0^2 z/2k\} . \quad (9)$$

The weighting factors B_j are found from the boundary condition $\mathcal{T}(\boldsymbol{R}, 0) = \exp\{i \boldsymbol{K}_0 \cdot \boldsymbol{R}\}$. The $\mathcal{T}_j(\boldsymbol{R})$ are suitably normalized solutions of

$$[\nabla_{\boldsymbol{R}}^2 + s_j^r - U^r(\boldsymbol{R})]\, \mathcal{T}_j(\boldsymbol{R}) = 0 . \quad (10)$$

Conservation of total energy (i. e., kinetic plus potential) for elastic scattering relates the eigenvalues s_j^r to the solutions $\boldsymbol{K}_j$ of Equations (2). To a good approximation, we find that

$$s_j^r = 2 k_0 [k_0 - |\boldsymbol{K}_j|] + \Delta . \quad (11)$$

A constant parameter Δ is introduced to allow the zero of s_j^r to be re-defined, as described below.

As already stated, the derivation of the dispersion Eqs. (2) requires that the inelastic waves are weak compared to the elastic waves, so that we are justified in using first order perturbation theory to find the imaginary parts of the eigenvalues. Thus replacing s_j^r by $(s_j^r + i s_j^i)$, we find

$$s_j^i = \int \mathrm{d}\boldsymbol{R}\, |\mathcal{T}_j(\boldsymbol{R})|^2 U^i(\boldsymbol{R}) \quad (12)$$

where the integral extends over the two dimensional unit cell in the $\boldsymbol{R}$-plane. These imaginary parts s_j^i are negative, because $\bar{U}^i(\boldsymbol{R})$ is negative.

We now limit the theory to crystals with one atom per fundamental unit cell, and to the one dimensional systematics case for which $\bar{U}(\boldsymbol{R})$ depends only on $\varkappa$, and can be written as $\bar{U}(\varkappa)$. The origin of the unit cell is mid-way between atomic planes (Figure 2). The zero of $\bar{U}^r(\varkappa)$ is defined to lie at the top of the potential barrier, so that Δ in Eq. (11) is $(2 m e/\hbar^2)\, [\sum_h (\mathcal{V}_{2h} - \mathcal{V}_{2h-1})]$. This choice for representing the real potential means that quasi-bound states have $s_j^r < 0$, while nearly free states have $s_j^r > 0$. It differs from the scheme suggested by Humphreys and Fisher [15] as being convenient for use in a conventional Bloch wave approach [8]. The imaginary part $\bar{U}^i(\varkappa)$ is referred to zero outside the crystal, in order to retain the correct normal absorption.

It was shown in I that the WKB approximation to $\mathcal{T}_j(\varkappa)$ for $s_j^r > 0$ is

$$\mathcal{T}_j^{\pm}(\varkappa) = \frac{\exp\{i \Phi(0, \varkappa; s_j^{r\pm})\}}{[s_j^{r\pm} - \bar{U}^r(\varkappa)]^{1/4} \left[2 \int_{-a/2}^{0} \frac{\mathrm{d}\varkappa}{[s_j^{r\pm} - \bar{U}^r(\varkappa)]^{1/2}}\right]^{1/2}} . \quad (13)$$

The $\pm$-signs refer to forward- and back-travelling wave solutions. The classical phase integral $\Phi(0, \varkappa; s_j^r)$ appearing in Eq. (13) is given by

$$\Phi(0, \varkappa; s_j^r) = \int_0^{\varkappa} [s_j^r - \bar{U}^r(\varkappa)]^{1/2} \mathrm{d}\varkappa . \quad (14)$$

A similar though slightly more complicated expression for $\mathcal{T}_j(\varkappa)$ is given for $s_j^r < 0$ [I, Eq. (69)]. In our present problem, these $\mathcal{T}_j(\varkappa)$ are eigenfunctions of the unperturbed Hamiltonian $[-\mathrm{d}^2/\mathrm{d}\varkappa^2 + \bar{U}^r(\varkappa)]$. Using the obvious one-dimensional equivalent of Eq. (12), the s_j^i are given approximately for both positive and negative s_j^r by

$$s_j^i = \mathrm{Re} \int_0^{a/2} \frac{\mathrm{d}\varkappa\, \bar{U}^i(\varkappa)}{[s_j^r - \bar{U}^r(\varkappa)]^{1/2}} \Big/ \mathrm{Re} \int_0^{a/2} \frac{\mathrm{d}\varkappa}{[s_j^r - \bar{U}^r(\varkappa)]^{1/2}} . \quad (15)$$

The "real part" notation ensures that for $s_j^r < 0$, only the classically accessible region, for which $s_j^r > \bar{U}^r(\varkappa)$, contributes to the integral. Figure 3 shows s^i as a continuous function of s^r for gold (111) systematics at 600 kV. The points corresponding to the real and imaginary parts of the eigen-

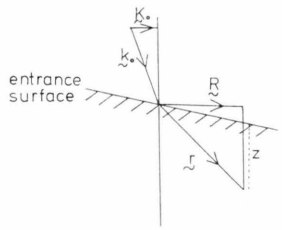

Fig. 1. Definitions of axes and of K_0.

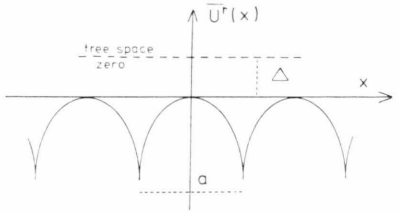

Fig. 2. The one dimensional potential $U^r(x)$. Real eigenvalues are defined relative to the top of the barrier. This choice for zero differs from zero potential energy in free space (the dotted line) by $\Delta = (2\,m\,e/\hbar^2)\,\Sigma\,(V_{2h}-V_{2h-1})$.

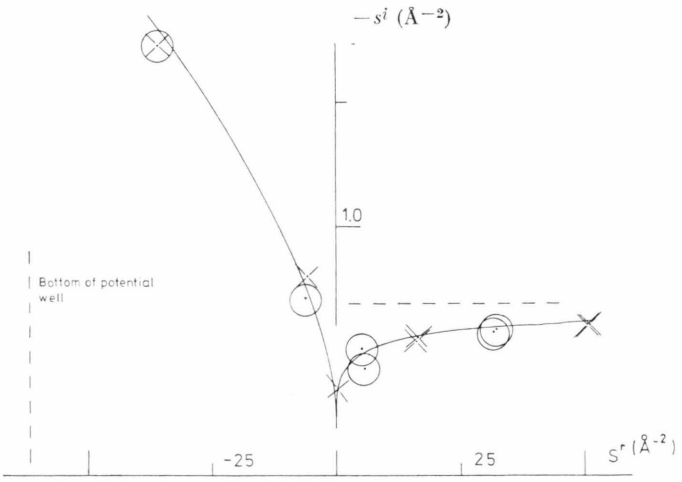

Fig. 3. The imaginary part s^i of the eigenvalue as a function of the real parts s^r, for gold (111) systematics at 600 KV. The real potentials used are based on the scattering factors of Doyle and Turner [15a], with Debye-Waller correction. The complex potential used is that suggested by Steeds [16]. The corresponding eigenvalues from 21 beam matrix calculations are shown for zero tilt (crosses) and for the first Bragg angle satisfied (circles). The limiting value for large s^r (the dotted line) is proportional to the mean absorption coefficient.

values found using conventional 21 beam matrix calculations [16] are also shown for two orientations. Agreement is good, demonstrating the validity of using WKB approximations for $\mathcal{T}_j(z)$ to find s_j^i. The eigenfunctions used to derive Eq. (15), such as those of (13), are not valid very close to $s^r=0$, as discussed in I, § 4. Therefore, the logarithmically sharp drop at $s^r=0$ in Fig. 3 may not precisely represent the analytic behaviour of s^i.

4. Penetration

The simplicity of Eq. (15) makes possible a description of electron penetration through thick specimens. We shall first establish the variation of s_j^r with energy. The s_j^r are given semi-classically (I) by the solutions of

$$|T(s)|\cos K_0 a = \cos\,[\mathrm{Re}\,\Phi(-a/2, a/2; s)] \quad (16)$$

where $T(s)$ is the coefficient for transmission through a single potential barrier (Figure 2). As voltage increases, the increase of $-\bar{U}^r(z)$ in Eq. (14) with the relativistic mass means that Φ increases, so that the solutions s_j^r of Eq. (16) decrease monotonically. Eigenvalues found in this way agree well with those from matrix calculations, as shown by Steeds and Enfield [17].

The penetration at a given energy is usually determined by the most strongly channeled wave, that

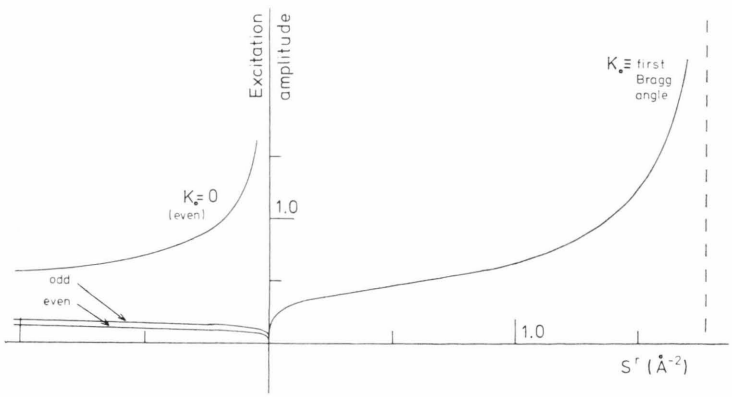

Fig. 4. The excitation amplitudes for the central beam for two orientations of gold (111) systematics at 600 KV, as a function of s^r. The same potentials are used as for Figure 3. Note the dependence on the symmetry for bound Bloch states. Antisymmetric bound states are not excited for $K_0=0$.

is by the state m with the minimum value of s^i, since for thick crystals, its contribution is exponentially large compared to contributions from other states [18]. Physically, optimum channeling arises when the wave $\mathcal{T}_m(\varkappa)$ most nearly avoids the atomic planes, and as seen on Fig. 3, this occurs at $s^r=0$ where the classical turning points [at which $\mathcal{T}_m(\varkappa)$ is large] come together midway between the atomic planes. For large z, provided B_m does not vanish, we can write

$$\mathcal{T}(\varkappa,z)\cong B_m\,\mathcal{T}_m(\varkappa)\,\exp\{-i(s_m{}^r+i\,s_m{}^i)\,z/2\,k\}\cdot\exp\{i\,K_0{}^2\,z/2\,k\}\,. \tag{17}$$

Equation (17) shows that the greatest penetration is achieved when $-s_m{}^i/k$ is a minimum, which occurs for $s_m{}^r$ slightly less than zero. This represents a compromise between optimum channeling, which occurs when $s_m{}^i=0$, and the decrease of both $1/k$ and of $\mathcal{V}_g{}^i$ with increasing E, as described below. We therefore only need to discuss quasi-bound states, for which the energy bands are narrow, that is to say $s_j{}^r$ – and hence $s_j{}^i$ – depend little on K_0, so that the best orientation is that for which the state m is most strongly excited. The excitation amplitude for forward scattering, found numerically using I, Eq. (88), is shown in Fig. 4 for normal incidence $K_0=0$ and for the first Bragg angle $K_0=\pi/a$, for gold(111) systematics at 600 kV. Bound states contribute more strongly for $K_0=0$. To illustrate analytically that $K_0=0$ is more suitable than any other orientation, we approximate the real potential by the parabola

$$\bar{U}^r(\varkappa)\cong -4\,|\,\bar{U}^r(a/2)\,|\,\varkappa^2/a^2. \tag{18}$$

Equation (18) gives the correct shape near the barrier top, which is the important region for this discussion. Using Eq. (18) and Eq. (88) of I for the excitation, it follows that the contribution from a state j to the diffracted beam G is principally determined by $f(s_j{}^r,K_0,K_G)$ where $K_G=K_0+G$, and

$$f(s_j{}^r,K_0,K_G)=[((K_0{}^2-s_j{}^r)\,(K_G{}^2-s_j{}^r))^{1/4}\ln(4\,|\,\bar{U}^r(a/2)\,|\,/\,|\,s_j{}^r\,|)]^{-1}. \tag{19}$$

This function reproduces the qualitative features of Figure 4. Clearly, a state with $s_j{}^r<0$ contributes most strongly, particularly to bright field, when $K_0=0$.

The lowest state ** $j=1$ is heavily absorbed for gold(111) systematics, as for example at 600 kV on Figure 3. The second state, which is antisymmetric for $K_0=0$, is not excited for this orientation. Therefore, the first voltage for optimum penetration is when $s_3{}^i/k$ is a minimum.

We must now test this account of the origin of the voltage for best penetration, E_m, by comparison with standard many beam calculations, such as those by Humphreys [19]. He used 21 systematic beams, with Debye-Waller corrected $\mathcal{V}_g{}^r$ values based on the scattering factors of Smith and Burge (l. c. [20]). We have repeated some of these calculations, and obtained the set of real eigenvalues. To find s^i/k against E, we need only use Eq. (15) at one reference voltage, say 100 kV, by constructing a "universal curve" in the following way.

In contrast to $\mathcal{V}_g{}^r$, which is independent of the electron velocity w, $\mathcal{V}_g{}^i$ varies approximately as the inverse of w as the incident energy eE is changed (see e. g. Hirsch [21]). Using this together with Equation (6),

$$\bar{U}_E{}^i(\varkappa)=\frac{\beta_{100}\sqrt{1-\beta_{100}{}^2}}{\beta_E\sqrt{1-\beta_E{}^2}}\,\bar{U}_{100}{}^i(\varkappa)\equiv\alpha(E)\,\bar{U}_{100}{}^i(\varkappa) \tag{20}$$

where $\beta_E=w/c$ is the usual relativistic parameter. Writing $s'\sqrt{1-\beta_{100}{}^2}=s^r\sqrt{1-\beta_E{}^2}$, Eqs. (15) and (20) give

$$s^i(s^r,E)/\alpha(E)=s^i(s',100) \tag{21}$$

Humphreys [19] used $\mathcal{V}_g{}^i$ values given by Humphreys and Hirsch [22]. These latter authors only give $\mathcal{V}_g{}^i$ values for small g. However, we can use the tables of Radi [23], since he also took an Einstein model for the thermal contribution, which largely determines $\mathcal{V}_g{}^i$ for higher-order g values. The different values for $g=0$ do not alter the shape of curves like that in Fig. 3, so that the value of E_m is not affected.

The function $s^i(s^r,E)/k$ can be written as

$$s^i(s^r,E)/k=(R/\beta_E{}^2)\;s^i(s',100) \tag{22}$$

where $R=\beta_{100}{}^2/k_{100}=1.77\times10^{-3}$ Å. Figure 5 shows $s^i(s',100)$ against s', using the $\mathcal{V}_g{}^i$ values of Radi [23] for gold (111) systematics at 100 kV. Given $s_3{}^r(E)$ for some E from the matrix calculations, s' is calculated and $s^i(s',100)$ is read from Figure 5. Equation (22) then gives $s^i(s^r,E)/k$, which is plotted as a function of E in Figure 6. The voltage E_m (=900 kV) for which this curve is a minimum agrees well with the value of E_m given by Humphreys [19], whose graph of penetration against E is reproduced in Figure 6.

** The lowest state in the notation used in I is $j=0$.

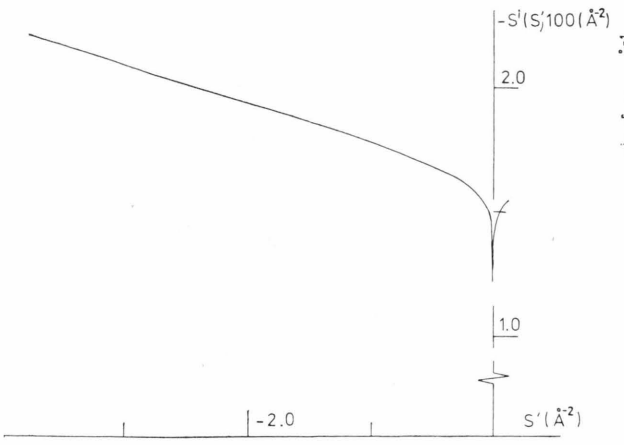

Fig. 5. The curve of s^i (s', 100) against s', which is valid for all energies, for gold (111) systematics.

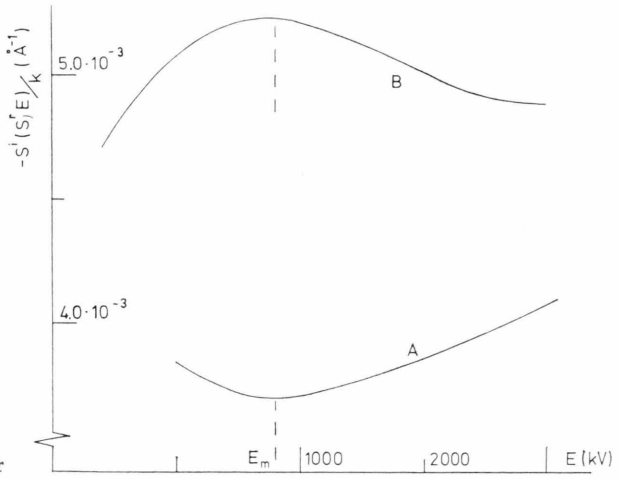

Fig. 6. Curve A is $s^i(s^r, E)/k$ against E for gold (111) systematics. Curve B reproduces the penetration in arbitrary units against E as calculated by Humphreys [19].

We have seen that for normal incidence, the penetration increases with voltage up to E_m. As the voltage is raised past E_m, the state $j=3$ continues to become more tightly bound, and the penetration decreases. At much higher voltages, the state $j=5$ becomes bound, and another peak of penetration is reached. The best penetration for voltages between these two peaks may occur for different orientations, since free states can be excited provided $s^r < K_0^2$, as shown in I using semiclassical approximations. Humphreys [19] has studied certain other orientations numerically. Whether or not penetration is greater for the $j=5$ peak than for the $j=3$ peak is determined by the voltage dependence of the $\mathcal{V}_g{}^i$ values, for which we have employed only a first approximation, but it appears that little increase in penetration is likely to result from going to the much higher voltage. For lighter materials, or for gold oriented for a weaker set of systematic reflections, higher values of E_m would be obtained.

[1] J. M. Cowley and A. F. Moodie, Acta Cryst. **10**, 609 [1957].
[2] F. Fujiwara, J. Phys. Soc. Japan **14**, 1513 [1959].
[3] K. Fujiwara, J. Phys. Soc. Japan **16**, 2226 [1961].
[4] F. Fujimoto, J. Phys. Soc. Japan **14**, 1558 [1959].
[5] Y. H. Ohtsuki and S. Yanagawa, J. Phys. Soc. Japan **21**, 326 [1966].
[6] M. V. Berry, J. Phys. C, Solid St. Phys. **4**, 697 [1971].
[7] K. Molière, Ann. Phys. Leipzig (5) **34**, 461 [1939].
[8] P. B. Hirsch, A. Howie, R. B. Nicholson, D. W. Pashley, and M. J. Whelan, Electron Microscopy of Thin Crystals, Butterworths, London 1965.
[9] G. Borrmann, Phys. Z. **42**, 157 [1941].
[10] G. Borrmann, Z. Phys. **127**, 297 [1950].
[11] H. Yoshioka, J. Phys. Soc. Japan **12**, 618 [1957].
[12] G. Radi, Z. Phys. **212**, 146 [1968].
[13] K. Ohtaka, Y. H. Ohtsuki, and S. Yanagawa, J. Phys. Soc. Japan **23**, 566 [1967].
[14] J. M. Cowley and A. F. Moodie, J. Phys. Soc. Japan **17**, Suppl. B-II, 86 [1962].
[15] C. J. Humphreys and R. M. Fisher, Acta Cryst. **A 27**, 42 [1971].
[15a] P. A. Doyle and P. S. Turner, Acta Cryst. **A 24**, 390 [1968].
[16] J. W. Steeds, Phys. Stat. Sol. **38**, 203 [1970].
[17] J. W. Steeds and A. Enfield, Electron Microscopy and Analysis, Inst. of Phys., p. 126 [1971].
[18] C. J. Humphreys, L. E. Thomas, J. S. Lally, and R. M. Fisher, Phil. Mag. **23**, 87 [1971].
[19] C. J. Humphreys, Phil. Mag. **25**, 1459 [1972].
[20] G. H. Smith and R. E. Burge, Acta Cryst. **15**, 182 [1962].
[21] P. B. Hirsch, J. Phys. Soc. Japan **17**, Suppl. B-II, 143 [1962].
[22] C. J. Humphreys and P. B. Hirsch, Phil. Mag. **18**, 115 [1968].
[23] G. Radi, Acta Cryst. **A 26**, 41 [1970].